Organic Electronics 13 (2012) 498–505

Contents lists available at SciVerse ScienceDirect

Organic Electronics

journal homepage: www.elsevier.com/locate/orgel

Fluorinated alkyl phosphonic acid SAMs replace PEDOT:PSS in polymer semiconductor devices

Mingqing Wang, Ian G. Hill *

Department of Physics, Dalhousie University, Halifax, NS, Canada B3H 4R2

ARTICLE INFO

Article history:
Received 22 June 2011
Received in revised form 28 November 2011
Accepted 4 December 2011
Available online 31 December 2011

Keywords:
Self-assembled monolayers
Fluorinated alkyl phosphonic acid
Work function
Hole injection
White PLED

ABSTRACT

Fluorinated phosphonic acids were self-assembled to form monolayers (SAMs) on indium tin oxide anodes, resulting in work functions that are 0.15–0.4 eV larger than PEDOT:PSS by Kelvin probe. X-ray photoelectron spectroscopy and water contact angle measurements were used to study monolayer growth kinetics and to verify the degree of coverage. Hole-only devices and white polymer light emitting diodes were constructed using unmodified ITO, SAM-modified ITO, and PEDOT:PSS on ITO to investigate the influence of the fluorinated SAMs on hole injection. Hole-only devices indicate improved hole injection compared to PEDOT:PSS. Compared with light-emitting diodes using pure ITO anodes, the SAM-modified devices show improved charge injection and ten times higher luminous efficiency. Compared to devices using PEDOT:PSS, SAM-modified devices show improved brightness and luminous efficiency, although with a slightly larger turn-on voltage. These materials are therefore suitable candidates to replace PEDOT:PSS as a hole injection layer in PLEDs.

In organic electronic devices including organic light-emitting diodes (OLEDs), polymer light-emitting diodes (PLEDs), organic field effect transistors (OFETs) and organic photovoltaics (OPVs), the interfaces between electrodes and organic materials greatly affect device performance. Charge transfer at the electrodes of OLEDs and OPVs is often limited by the energy offsets between the frontier orbitals of the molecular components and the Fermi energies of the contacting electrodes. Indium–tin oxide (ITO) is widely used as transparent electrode in organic electronics. Various chemical and physical approaches have been used to modify the surface properties and work function of ITO. Spin coating a layer of poly(3,4-ethylenedioxythiophene)/poly(styrenesulfonate) (PEDOT:PSS) onto air/oxygen plasma etched, or UV/ozone cleaned ITO is the most widely used method at present. However, PEDOT:PSS is strongly acidic in nature, and can lead to degradation of the device, limiting its lifetime [1]. Another important approach to modify the surface properties and work function of ITO is the use of monolayers of dipolar molecules with various functional groups that can anchor to the surface, such as thiols, silanes, carboxylates, COCl, and SO_2Cl_2 [2–10]. Monolayers of these molecules on the ITO surface can result in an effective dipole moment at the interface that modifies the work function of ITO, thereby impacting charge injection into the device. Recently, the use of phosphonic acid SAMs was motivated by their superior bonding ability with hydroxyl terminated metal oxide materials like ITO [11–15]. Modification of ITO with a partially fluorinated phosphonic acid has been reported to improve the efficiency and lifetime of small molecule organic light emitting devices (OLEDs) [16]. In small molecule OLEDs, organic materials are generally deposited by vacuum thermal deposition. Polymer OLEDs can be prepared by spin coating or ink-jet printing methods that are easy to process and suitable for large area, low cost production. PLEDs that can emit white light are of particular interest and potentially important for use in active-matrix displays (using color filters) and solid-state lighting.

* Corresponding author.
E-mail address: ian.hill@dal.ca (I.G. Hill).

1566-1199/$ - see front matter © 2012 Elsevier B.V. All rights reserved.
doi:10.1016/j.orgel.2011.12.008

In this paper we report on the application of a fluorinated alkyl phosphonic acid SAM to an ITO anode and its effect on the work function and surface energy of ITO as well as its influence on hole injection into polymeric semiconductor films. As a further demonstration, the electronic and optical properties of white light emitting PLEDs incorporating these monolayers were studied. Fluorinated molecules were chosen due to their strong electron withdrawing nature. Shifting of some electron density from the ITO to the SAM molecules will result in an interface dipole of the sense that will increase the energy required of an electron to escape the surface of the modified ITO, therefore increasing its work function. Unfortunately, the wetting of materials deposited on fluorocarbons is typically poor, influencing the choice of materials/solvents used in the first layer to be spin coated on the SAM. Furthermore, PEDOT:PSS serves not only as a hole injection layer in a typical PLED, but also to some degree as an electron blocking layer, preventing electrons from traversing the device without combining with holes to form excitons. While it has been reported that PEDOT:PSS is not an ideal electron blocker [17], it was anticipated that a single molecular layer would be even less efficient. Furthermore, it is desirable to spatially separate the recombination zone of the emissive layer from the ITO electrode to avoid non-radiative recombination paths available to excitons through the dipole-dipole interaction near a metallic electrode [18]. To address all of these issues, we have introduced a thin film of poly(N-N′-bis(4-butylphenyl)-N,N′-bis(phenyl)benzidine) (poly-TPD) as hole transport layer/electron blocking layer. It was found that poly-TPD reliably wet the shorter chain SAM-modified ITO surfaces.

The chemical structures of 3,3,4,4,5,5,6,6,6-fluorohexylphosphonic acid (FHPA) , 3,3,4,4,5,5,6,6,7,7,8,8,8-fluorooctylphosphonic acid (FOPA) and 3,3,4,4,5,5,6,6,7,7,8,8, 9,9, 10,10,11,11,12,12,12-fluorododecylphosphonic acid (FDPA) are shown in Fig. 1 FHPA, FOPA and FDPA were purchased from Specific Polymers. ITO coated glass substrates (20 Ω/square; Delta Technologies) were first cleaned in an ultrasonic bath using a dilute solution of Triton-X in de-ionized (DI) water for 20 min, followed by sonication for 20 min in DI water. Further cleaning was done by sonicating in acetone and then ethanol for 30 min. After solvent cleaning, ITO substrates were oxygen plasma ashed (250 mTorr, 150 W, 8″ parallel plate RIE) for 2 min.

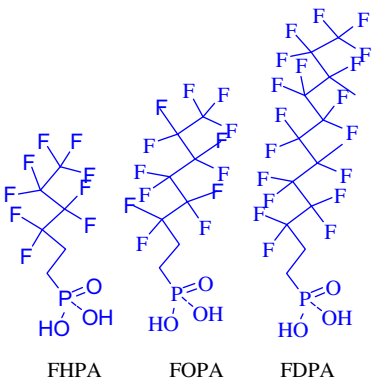

Fig. 1. Molecules used for SAM modification of ITO.

The procedure for SAM assembly was as follows. After plasma ashing, the ITO slides were immersed in a 1 mM ethanol/chloroform (V:V = 1:2) solution of the corresponding phosphonic acid for 12 h. The ITO substrate was then rinsed with ethanol and DI water, sonicated in absolute ethanol to remove any multilayer material, and transferred to a vacuum oven where it was baked at 140 °C for 2 h to achieve complete chemical bonding.

The influence of the SAM surface treatments on the work function of ITO is shown in Table 1. Work functions were measured via Kelvin probe in air. Note that Kelvin probe does not measure the absolute work function, but rather the contact potential difference relative to the probe. Although there is a large uncertainty in the actual value of the work function, relative changes in work function between different samples can be measured very accurately. The reported work function values were determined by assuming the work function of a reference Au sample to be 5.2 eV. A bare, oxygen-plasma treated ITO sample showed an average work function of 4.7 eV, consistent with earlier reports [19]. PEDOT:PSS covered ITO showed a work function of 5.2 eV. ITO modified with FOPA and FHPA exhibited work functions of 5.36 eV and 5.42 eV, respectively. ITO modified with FDPA exhibited a work function of 5.6 eV. Again, we stress that it is not the absolute, but the relative changes in work function that are important to this study. The large increase in the work function for SAM modified ITO can be attributed to the surface dipole pointing away from the surface caused by the electronegative fluorine substituents. Another important aspect of this interface modification is its impact on the surface energy of ITO. The measured contact angles with water for FHPA, FOPA and FDPA were 106°, 108° and 111°, respectively (see Table 1). The higher contact angles for phosphonic acid modified ITO indicate a more hydrophobic surface that is expected to be more compatible with generally hydrophobic organic layers. However, part of the reason for including the poly-TPD layer was to provide a surface that would allow better wetting of the luminous layer, due to the generally poor wetting of both hydrophobic and hydrophilic materials on fluorocarbons. Using FDPA SAM-modified ITO, with the longest fluorocarbon chain and most hydrophobic surface, we were unable to achieve sufficient wetting of the poly-TPD layer to fabricate reliable PLEDs. However, uniform films of poly-TPD were reliably formed on both FHPA and FOPA SAMs.

To better understand the kinetics of monolayer growth in this system, and to confirm the presence of a near-saturated monolayer, both contact angle and X-ray

Table 1
Contact angle and work function of different SAM modified ITO glass.

Sample	Contact angle with water (°)	Work function (eV)
ITO	42.42	4.72
PEDOT	28.57	5.21
FHPA	106.11	5.36
FOPA	108.67	5.42
FDPA	110.55	5.63

photoelectron spectroscopy (XPS; Mg Kα, $h\nu$ = 1253.6 eV) were performed on samples immersed in the SAM solutions for times ranging from 0 min to over 2000 min. The XPS data for In 3d, F 1s, Sn 3d, C 1s, O 1s, and P 2p core levels were studied. Fig. 2 illustrates typical F 1s and In 3d spectra from a sample immersed for 1027 min in 1 mM FHPA in ethanol/chloroform. The F1s data are simply fit with a single pseudo-Voigt function and a Shirley background. The In 3d data are slightly more complicated, in that 2 pseudo-Voigt functions are required for both the J = 3/2 and J = 5/2 peaks. The areas were constrained to the expected 2:3 ratio, due to the degeneracy of the states, and resulted in excellent fits to the experimental data. We hypothesize that these correspond to surface and bulk species with slightly different

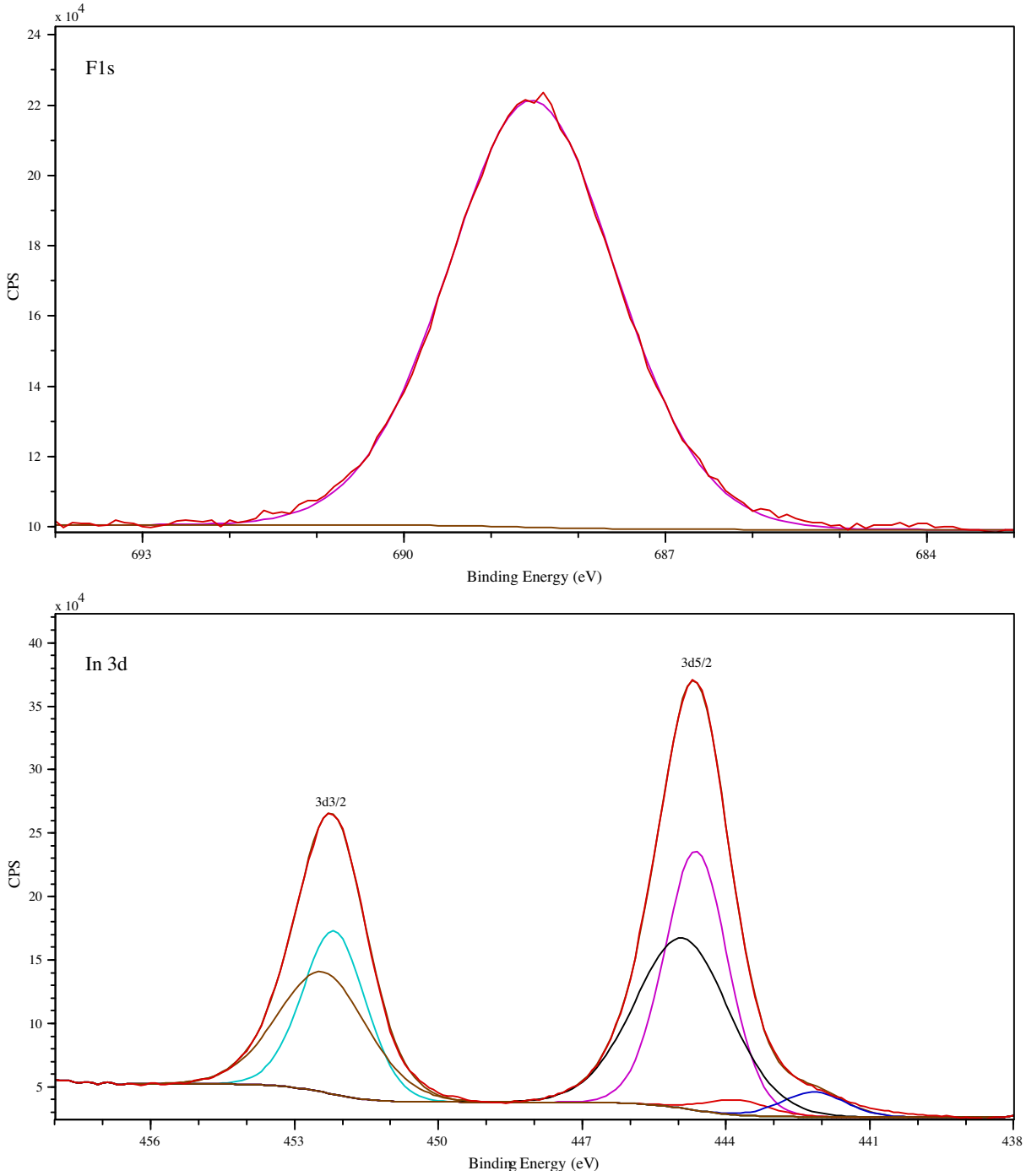

Fig. 2. F 1s and In 3d core level XPS spectra for an ITO sample immersed in 1 mM FHPA for 1027 min.

binding energies. In addition, two small peaks on the low binding energy edge of the $J = 5/2$ peak were included. These correspond to $J = 3/2$ electrons excited by satellite emission from Mg $K\alpha_3$ and $K\alpha_4$.

To determine the evolution of the fractional monolayer coverage with immersion time, the ratio of the F 1s to In $3d_{5/2}$ peak areas was analyzed. The ratio, rather than simply the F 1s intensity, was used to minimize experimental uncertainties caused by sample positioning, X-ray source positioning, surface roughness and inevitable sample contamination from the air, all of which would affect the relative count rate of different samples. The ratios of F 1s to In $3d_{5/2}$ intensities for various immersion times are presented in Fig. 3. Also included in the figure are the expected ratios for two models of monolayer growth, including attenuation of the In 3d intensity due to the growth of the overlayer: Langmuir kinetics, where the rate of molecular deposition is proportional to $(1 - \chi)$, where χ is the monolayer fractional coverage, and a combination of partial Langmuir–Blodgett deposition and diffusion limited growth proposed by Woodward et al. [20] for the growth of octadecylphosphonic acid (ODPA) on mica. In the latter model, the molecular coverage is the result of two processes: a partial quasi-Langmuir–Blodgett (LB) film which forms when the substrate is removed and withdrawn through the surface of the solution, and a film that deposits while the sample is immersed, the kinetics of which are limited by a diffusion-like process. The most significant prediction of this model is that a significantly higher than expected coverage occurs for short time scales due to the LB contribution. This is exactly what was found here.

The simulated ratios for Langmuir kinetics are calculated using a time constant of 60 min, but do not reproduce the data for any value of the time constant. For the LB/diffusion model, a value of λ (the fractional coverage due to the quasi-LB contribution for 0 immersion time) of 0.35, and a value of T_D, the timescale of diffusive transport, of 10 min were used, and reproduce the data quite well. Although care must be taken comparing our results for FHPA in ethanol/chloroform deposited on ITO with the data of Woodward et al. for ODPA in THF deposited on mica, it is interesting to note that a T_D of 600 s is comparable to the range of 600–1200 s reported for 1 mM ODPA and other acid-based SAMS [20,21], and λ of 0.35 reported here is larger than, but comparable to the values of 0.15–0.25 reported for 1 and 2 mM ODPA. One might expect the fraction of the fluorinated species segregated at the surface of the solution to be larger than the non-fluorinated ODPA, resulting in a larger fraction of a monolayer deposited by the quasi-LB mechanism for the fluorinated vs the non-fluorinated species.

Due to the quasi-LB contribution discussed above, even samples immersed for very short times contain a significant fraction of a monolayer coverage. As such, the static water contact angle increase from 42° to 99° after just 1 min of immersion. Longer immersion times result in a contact angle that saturates at 106°, as shown in Fig. 4. Note that the contact angle has been plotted as a function of fractional coverage derived from the XPS measurements. Following Woodward et al. [22] the cosines of the static water contact angles are plotted in the second frame of Fig. 4. Although we lack data a low coverages, our data appear to agree with those of Woodward et al. where two regions were identified; the first, with rapid change below a fractional coverage of 0.5 and the second, a much slower change above 0.5. This characterization of the monolayer growth kinetics, and especially the strong similarities to the results reported previously for ODPA on mica, allow us to conclude with high confidence that our 720 min immersion time for samples used in devices results in films containing very close to a saturated monolayer, with a fractional coverage in excess of 0.95.

For the fabrication of white-emitting PLEDs, we dissolved poly-TPD and PFO doped with 0.2% (w/w) MEH-PPV in chlorobenzene and toluene, respectively. Selective

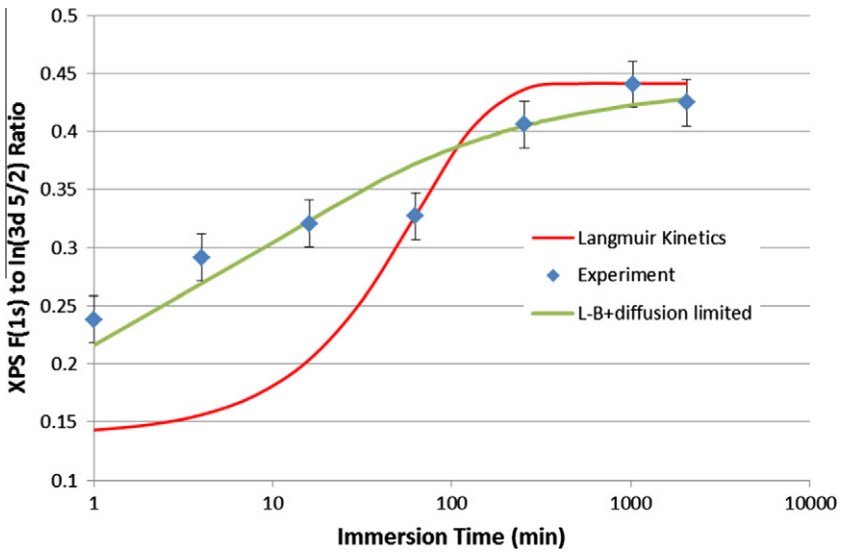

Fig. 3. Ratio of the F 1s to In $3d_{5/2}$ intensities for various immersion times in 1 mM FHPA. The red line is the predicted ratio for Langmuir adsorption kinetics with a time constant of 60 min. The green line is the predicted ratio for a quasi-LB/diffusion limited kinetics model after ref 20.

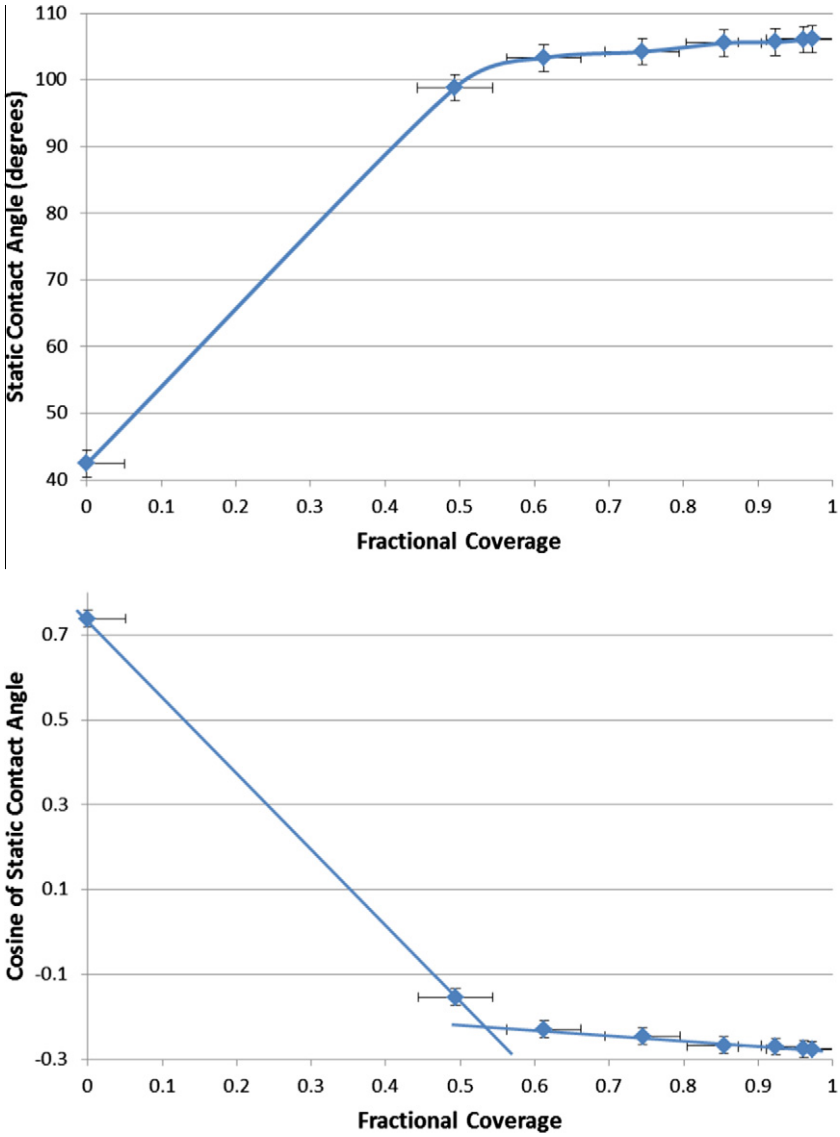

Fig. 4. Static water contact angle (top) and cosine (bottom) as a function of fractional monolayer coverage of FHPA on ITO.

solubility allowed us to deposit the luminous layer without dissolving the underlying hole transport layer by sequential spin coating. After spin coating, poly-TPD and PFO/MEH-PPV were annealed at 120 °C and 75 °C, respectively for 30 min in a N_2 glove box. Fig. 5 shows the device structure and materials used in the PLEDs. Configurations of the devices were: ITO/ hole injection layer/poly-TPD (40 nm)/PFO:MEH-PPV (70 nm)/Ca (20 nm)/Al (70 nm), where the hole injection layer was PEDOT:PSS (30 nm) , FHPA, FOPA or was absent in the case of the control devices.

Fig. 6 shows the current–voltage, luminance–voltage and luminous efficiency–voltage characteristics of the devices. The Fermi level of O-plasma ITO is at −4.7 eV relative to the vacuum as determined by Kelvin probe and consistent with the literature [19], but the HOMO levels of PFO and MEH-PPV in the luminous layer are at −5.8 and −5.2 eV, respectively [23,24]. An energy level difference between the ITO anode and the luminous polymer as large as 1 eV is quite a large barrier for hole injection. Even the intermediate level of the poly-TPD HOMO at 5.1–5.4 eV [25,26] would result in a hole injection barrier as high as 0.7 eV at either the ITO/poly-TPD or poly-TPD/PFO interface. Depending on the true value of the poly-TPD ionization potential (IP), either the ITO/poly-TPD or poly-TPD/PFO interface will the rate determining step for hole injection. Larger values of the IP would imply the former and smaller the latter. Therefore, the *I–V* curve of untreated ITO/poly-TPD/PFO:MEH-PPV/Ca:Al PLED device exhibits low current density due to poor hole injection. In addition, we note large, unstable leakage currents at voltages below 5 V and low current density above 5 V. The luminous efficiency and intensity are also very low in PLEDs using bare ITO. The unstable leakage currents in the device could be associated with the presence of pin holes in the hole

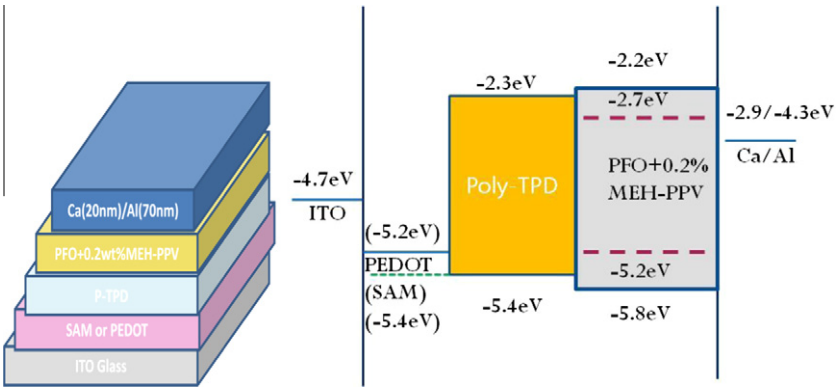

Fig. 5. Device structure and energy levels of the PLED materials.

transport poly-TPD layer or the luminous layer (PFO/MEH-PPV), perhaps due to poor wetting and non-uniform thickness of the poly-TPD on the hydrophilic O-plasma treated ITO surface. The lower current density above 5 V for bare ITO based PLEDs is a result of a large hole injection barrier either between ITO and the poly-TPD layer or between the poly-TPD and PFO. In contrast, the *I–V* curve of the device using FHPA SAM modified ITO shows greatly enhanced current densities. Improved hole injection in the FHPA SAM modified device as compared to the untreated ITO device can be attributed to the higher work function of the SAM modified ITO and the consequent lowering of the ITO/poly-TPD hole injection barrier. Note that this also implies that hole injection across the ITO/poly-TPD interface was the rate determining step, and not the poly-TPD/PFO interface, which remained unchanged. This would seem to indicate that the ionization potential of the poly-TPD is most likely closer to 5.4, rather than 5.1 eV.

After FHPA SAM modification, the work function of the ITO electrode was 5.36 eV. The presence of a FHPA SAM reduces the hole injection barrier and consequently lowers the turn-on voltage and enhances the quantum efficiency of the device. Devices utilizing ITO modified with FOPA exhibit *I–V* curves similar to those using FHPA modified ITO, consistent with the similar work function of the SAM modified ITO (5.42 eV compared to 5.36 eV; see Table 1). Fig. 6(b) and (c) show the luminance and luminous efficiency (cd/A) as functions of applied voltage for these devices. The turn on voltages for FOPA, FHPA, PEDOT:PSS, and untreated samples were, 4.7, 4.8, 4.3 and 9.8 V, respectively (see Table 2). The maximum luminous efficiency for FOPA, FHPA, PEDOT:PSS, and untreated samples were, 1.16, 0.95, 1.06 and 0.1 cd/A, respectively. Compared with devices using pure ITO, the SAM modified anodes show much lower turn on voltage and about ten times increased luminous efficiency. Compared with PLEDs using PEDOT:PSS, the turn-on voltage increased slightly from 4.3 eV to 4.8 eV for FHPA-modified devices and 4.7 eV for FOPA-modified devices. Nonetheless, the modification of the ITO with fluorinated alkyl-SAMs results in device performance comparable to that obtained using the PEDOT:PSS on ITO, without introducing a strongly acidic component to the hole injection layer.

In order to directly compare hole injection between SAM modified, PEDOT:PSS modified ITO and pure ITO anodes, the following hole-only devices were prepared: ITO/poly-TPD (60 nm)/Al (80 nm). The *I–V* characteristics of the devices are dominated by holes since the work functions of the anodes (4.7–5.4 eV) are close to the ionization potential of poly-TPD (5.4 eV), and that of the cathode (4.3 eV) is much larger than the electron affinity of poly-TPD (2.3 eV). As can be seen in Fig. 7, hole injection was very inefficient for the pure ITO anode, but the current was significantly enhanced by SAM or PEDOT:PSS modification. The FHPA SAM modified ITO based devices show higher current than devices based on FOPA SAM modified ITO. This may be due to the insulating nature of the fluorinated alkyl chain. The octyl chain presents a longer insulting barrier to injection.

When charge carriers are injected into an intrinsic semiconductor or an insulator, the electric field due to the net charge density near the injecting contact diminishes the applied field. If carrier injection is increased (by lowering the injection barrier), the field will eventually vanish at the contact and further reduction of the charge injection barrier will not increase the injected current. This is known as the space charge limit, and the corresponding material-dependent current density is known as the space charge limited current (SCLC) [27]:

$$J_{SC} = \left(\frac{9}{8}\right)\varepsilon\mu\left(\frac{V^2}{L^3}\right)$$

where μ is the charge carrier mobility, ε is the dielectric permittivity of the semiconductor, and L denotes the active layer thickness. If the contact barrier height is greater than 0.25–0.3 eV, the current is generally injection limited at room temperature [28]. At lower barriers, the current is transport limited, and cannot exceed the space charge limit.

In order to better understand the effect of SAM modification of ITO on charge injection and transport in the diodes, *I–V* curves of hole-only devices with and without SAM or PEDOT:PSS modification were measured as a functions of temperature from 273 to 323 K (Fig. 8). Also

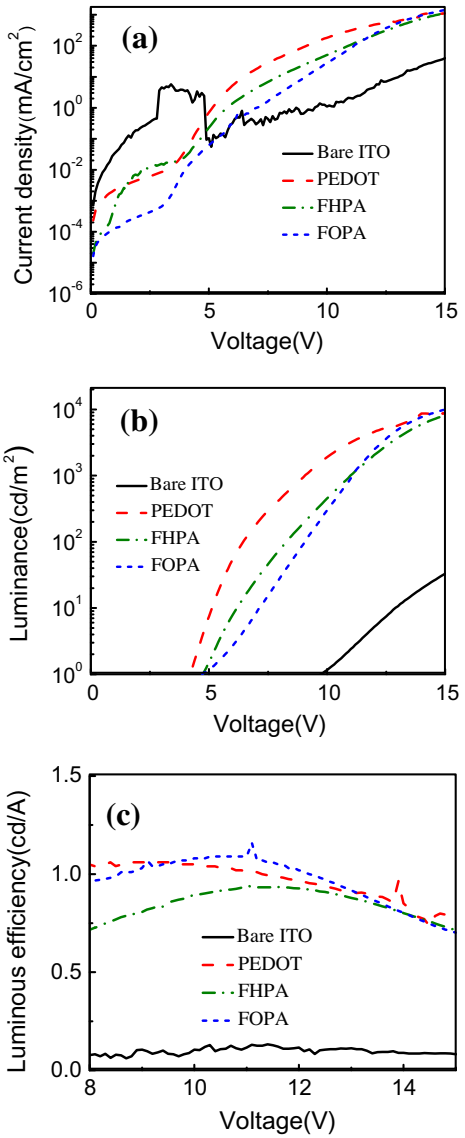

Fig. 6. Device characteristics of ITO/HIL/poly-TPD/PFO:MEH-PPV/Ca:Al with and without SAM or PEDOT:PSS modification: (a) current–voltage; (b) luminance voltage; (c) luminous efficiency–voltage.

Table 2
The turn on voltage ($L = 1$ cd/m^2), maximum luminance (at 15 V) and maximum efficiency (cd/A) of white PLEDs using different anodes.

Anode	Turn on voltage (V)	Maximum luminance (cd/m^2)	Maximum efficiency (cd/A)
ITO	9.8	33.1	0.1 (at 13.8 V)
ITO/PEDOT:PSS	4.3	8790	1.06 (at 8.8 V)
ITO/FHPA	4.8	8110	0.95 (at 11.0 V)
ITO/FOPA	4.7	10,000	1.16 (at 11.1 V)

plotted in Fig. 8 is the V^2 dependent SCLC (assuming a hole mobility of 10^{-3} cm^2/Vs) that would be expected if the systems were not injection limited. We note that the FHPA,

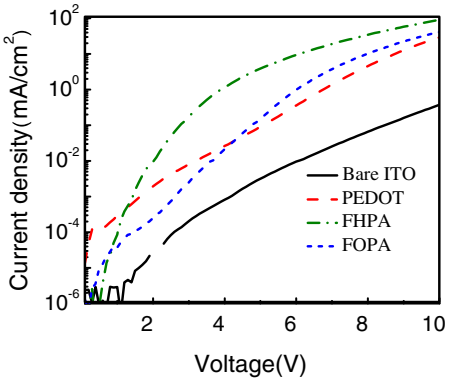

Fig. 7. *I–V* characteristics of hole only ITO/HIL/poly-TPD/Al devices with and without SAM or PEDOT:PSS modification.

FOPA and PEDOT-modified systems all appear to asymptotically approach this limit at high fields, and that the temperature dependence of the current is weaker at higher fields. This implies that these three systems are transitioning from injection limited to bulk limited conduction at high fields, but that all four systems are injection limited at lower fields. This transition can be qualitatively understood by the Schottky effect, which results in a field-dependent lowering of the charge injection barrier. In the three modified ITO systems, the hole injection barrier is sufficiently small at high applied bias that the system becomes space charge limited.

In conclusion, fluorinated alkyl phosphonic acid FHPA and FOPA were self-assembled to form monolayers on ITO anodes. The work functions and monolayer coverage of the modified ITO substrates were characterized using Kelvin probe, XPS and water contact angle measurements. The monolayer growth kinetics were described by a combination of quasi-LB and diffusion limited transport. An immersion time of 720 min was determined to produce a monolayer fractional coverage in excess of 95%. PLED devices based on bare, SAM-modified and PEDOT:PSS-modified ITO were fabricated. The SAM-modified devices showed much better charge injection and ten times higher luminous efficiency compared to bare ITO devices. The devices using SAM-modified ITO showed performance comparable to that obtained using PEDOT:PSS as a hole injection layer on ITO. These results are very promising when considering the selection of a surface modification technique in solution processable organic electronics. Future work will focus on improving the wetting characteristics of the SAM-modified surfaces, and the use of conjugated rather than aliphatic fluorocarbons. We also note that poly-TPD appears to act as an electron blocking layer comparable to PEDOT:PSS. The poly-TPD LUMO does not, however, present an energetic barrier to electrons from the PFO. A more suitable electron blocking layer may further enhance the luminous efficiency, resulting in another clear advantage over PEDOT:PSS. Temperature dependent *I–V* studies of hole-only poly-TPD single layer devices revealed all systems to be injection limited at low fields. The PEDOT:PSS, FHPA and FOPA/poly-TPD systems appear to approach SCLC at high fields due to Schottky injection

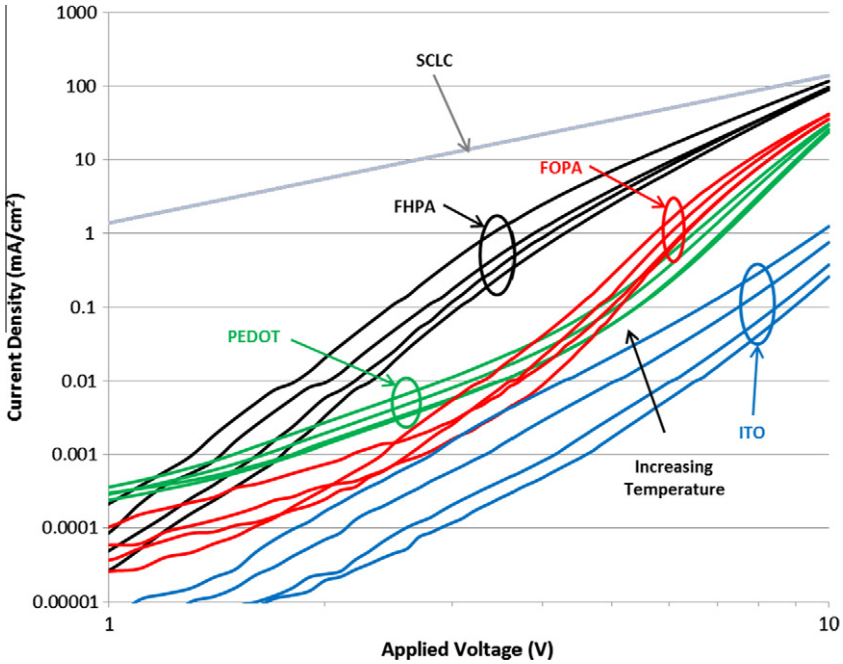

Fig. 8. *I–V* characteristics of the ITO/poly-TPD/Al devices with and without SAM or PEDOT:PSS modification at 273, 283, 303 and 323 K. The line varying as V^2 represents the bulk (trap free) space charge limit assuming a constant hole mobility of 10^{-3} cm^2/Vs.

barrier lowering, while the ITO/poly-TPD system appears injection limited throughout.

Acknowledgements

This research was funded by the Natural Sciences and Engineering Research Council of Canada and Canadian Foundation for Innovation and Springboard Atlantic. The authors would like to thanks Prof. Peng Zhang for use of his Kelvin probe facility.

References

[1] M.P. de Jong, L.J. van IJzendoorn, M.J.A. de Voigt, Appl. Phys. Lett. 77 (2000) 2255–2257.
[2] I.H. Campbell, S. Rubin, T.A. Zawodzinski, J.D. Kress, R.L. Martin, D.L. Smith, N.N. Barashkov, J.P. Ferraris, Phys. Rev. B. 54 (1996) 14321–14324.
[3] S. Khodabakhsh, D. Poplavskyy, S. Heutz, J. Nelson, D.D.C. Bradley, F. Murata, T.S. Jones, Adv. Funct. Mater. 14 (2004) 1205–1210.
[4] R.A. Hatton, S.R. Day, M.A. Chesters, M.R. Willis, Thin Solid Films 394 (2001) 292–297.
[5] E. L. Hanson, J. Guo, N. Koch, J. Schwartz, S.L. Bernasek, J. Am. Chem .Soc.127 (2005) 10058–10062.
[6] S.F.J. Appleyard, S.R. Day, R.D. Pickford, M.R. Willis, J. Mater. Chem. 10 (2000) 169–173.
[7] J. Lee, B.J. Jung, J.I. Lee, H.Y. Chu, L.M. Do, H.K. Shim, J. Mater. Chem. 12 (2002) 3494–3498.
[8] R.A. Hatton, M.R. Willis, M.A. Chesters, F.J.M. Rutten, D. Briggs, J. Mater. Chem. 13 (2003) 38–43.
[9] C.H. Yan, G.H. He, J.R. Zheng, Y.F. Li, Synth. Met. 121 (2001) 1343–1344.
[10] C.C. Hsiao, C.H. Chang, M.C. Hung, N.J. Yang, S.A. Chen, Appl. Phys. Lett. 86 (2005) 223505.
[11] S.A. Paniagua, P.J. Hotchkiss, S.C. Jones, S.R. Marder, A. Mudalige, F.S. Marrikar, J.E. Pemberton, N.R. Armstrong, J. Phys. Chem. C 112 (2008) 7809–7817.
[12] S.E. Koh, K.D. McDonald, D.H. Holt, C.S. Dulcey, J.A. Chaney, P.E. Pehrsson, Langmuir 22 (2006) 6249–6255.
[13] A. Sharma, P.J. Hotchkiss, S.R. Marder, B. Kippelen, J. Appl. Phys. 105 (2009) 084507.
[14] S. Besbes, H. Ben Ouada, J. Davenas, L. Ponsonnet, N. Jaffrezic, P. Alcouffe, Mater. Sci. Eng. C Biomimetic Supramol. Syst. 26 (2006) 505–510.
[15] S. Besbes, A. Ltaief, K. Reybier, L. Ponsonnet, N. Jaffrezic, J. Davenas, H. Ben Ouada, Synth. Met. 138 (2003) 197–200.
[16] A. Sharma, B. Kippelen, P.J. Hotchkiss, S.R. Marder, Appl. Phys. Lett. 93 (2008) 163308.
[17] A.W. Hains, J. Liu, A.B.F. Martinson, M.D. Irwin, T.J. Marks, Adv. Funct. Mater. 20 (2010) 595–606.
[18] B.K. Crone, P.S. Davids, I.H. Campbell, D.L. Smith, J. Appl. Phys. 84 (1998) 833–842.
[19] D. Milliron, I.G. Hill, A. Kahn, J. Schwartz, J. Appl. Phys. 87 (2000) 572–576.
[20] J.T. Woodward, I. Doudevski, H.D. Sikes, D.K. Schwartz, J. Phys. Chem. B 101 (1997) 7535–7541.
[21] D.K. Schwartz, Annu. Rev. Phys. Chem. 52 (2001) 107–137.
[22] J.T. Woodward, A. Ulman, D.K. Schwartz, Langmuir 12 (1996) 3626–3629.
[23] A.J. Campbell, D.D.C. Bradley, H. Antoniadis, Appl. Phys. Lett .79 (2001) 2133–2135.
[24] T. Yamanari, T. Taima, J. Sakai, K. Saito, Sol. Energy Mater. Sol. Cells 93 (2009) 759–761.
[25] S. Vaddiraju, M. Mathai, E. Kymakis, F. Papadimitrakopoulos, Chem. Mater. 19 (2007) 4049–4055.
[26] G. Sarasqueta, K.R. Choudhury, J. Subbiah, F. So, Adv. Funct. Mater. 21 (2011) 167–171.
[27] M.A. Lampert, P. Mark, Current Injection in Solids, New York, 1970.
[28] M. Pope, C.E. Swenberg, Electronic Processes in Organic Crystals and Polymers, second ed., Oxford University Press, Oxford, 1999.